Materials Science & Engineering A 650 (2016) 15–19

Contents lists available at ScienceDirect

Materials Science & Engineering A

journal homepage: www.elsevier.com/locate/msea

Evaluation of high-temperature Vickers hardness using instrumented indentation system

Chan-Pyoung Park [a,*], Jung-Jun Lee [a], Seung-Kyun Kang [b], Young-Cheon Kim [c], Kwan-Sik Woo [a], Seung-Won Jeon [a], Dongil Kwon [a]

[a] Department of Materials Science and Engineering, Seoul National University, Seoul 151-744, Republic of Korea
[b] Department of Materials Science and Engineering, Frederick Seitz Materials Research Laboratory, University of Illinois at Urbana-Champaign, Urbana, IL 61801, USA
[c] School of Materials Science and Engineering, Ulsan National Institute of Science and Technology (UNIST), Ulsan 689-798, Republic of Korea

ARTICLE INFO

Article history:
Received 4 September 2015
Received in revised form
8 October 2015
Accepted 9 October 2015

Keywords:
High-temperature instrumented indentation system
Frame compliance calibration
Vickers hardness
Surface contact area
Plastic pileup deformation

ABSTRACT

Instrumented indentation testing is more advanced than conventional hardness testing in measuring various mechanical properties of materials. To evaluate these mechanical properties, information about indentation contact area is required. In particular, the deformation behavior of metals at high-temperatures seems to differ from that at room temperature, and thus for accurate evaluation of mechanical characteristics at high-temperatures, the high-temperature contact area should be used. In this study, an instrumented indentation system for high-temperatures was developed and measurement-errors caused by equipment temperature were calibrated. In addition, the pileup effect during indentation was studied at different temperatures. A new equation for the high-temperature contact area is proposed. For verification, conventional hardness testing was performed to compare the results with high-temperature instrumented indentation testing.

1. Introduction

Instrumented indentation testing (IIT) improves on conventional hardness testing by allowing various mechanical properties to be evaluated by analysis of the load–depth curve during indentation. IIT has a simple procedure and the advantage of measuring a local area such as a weldment, so it has been used extensively to evaluate in-field safety of power and petrochemical plants [1–4]. In recent years, IIT has also evaluated not only hardness and elastic modulus but also strength, fracture toughness, and residual stress. Evaluating all these mechanical characteristics requires knowledge of the contact area [5–11]; this is obtained by measuring a penetration depth from the material surface in loading and reflects the geometrical shape of the indenter, whereas the contact area in conventional hardness testing is obtained by observing the indentation mark [1,2].

Studies to determine contact area have performed through finite element analysis or experiments considering the elastic–plastic behavior of several materials. However, most of these studies have been limited to room temperature [12–16]; the high-temperature contact area has been determined by using the equation developed at room temperature or a modified equation reflecting high-temperature effects. The difficulty is that most high-temperature studies entail development and calibration of equipment. In addition, previous studies have been performed on the nano scale and at relatively low temperatures, usually below 200 °C [17–21].

In this study, a high-temperature instrumented indentation system (HTIIS), available on macro scale up to 650 °C, was developed. In addition, frame compliance (C_{frame}), i.e. the mechanical measurement-errors occurring at high-temperatures, was calibrated. To determine the contact area accurately using this new equipment, the pileup phenomenon occurring around the contact area during indentation, was quantified and its physical meaning was analyzed. A new calibration factor $f_{(T)}$ is suggested to correct for the pileup effect at high-temperatures, and conventional high-temperature Vickers testing was conducted to verify the reliability of HTIIS and the contact area from $f_{(T)}$.

2. Experiments

To carry out the high-temperature indentation experiments, a high-temperature chamber was constructed and IIT equipment was attached. The inside of the chamber contained a halogen lamp, thermocouples and stage. Specimen oxidation and thermal

* Corresponding author. Fax: +82 2 886 4847.
E-mail address: pchp@snu.ac.kr (C.-P. Park).

http://dx.doi.org/10.1016/j.msea.2015.10.034
0921-5093/

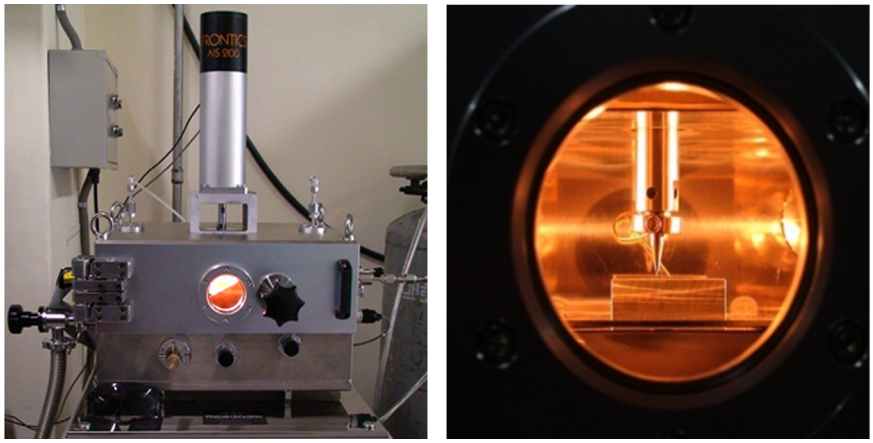

Fig. 1. Structure of HTIIS.

Table 1
Specifications.

	Specification		
IIT	Load	Maximum	300 kgf
		Resolution	5.6 gf
	Depth	Stroke	40 mm
		Resolution	0.1 um
	IIT shaft	Length	192 mm
H.T chamber	Vacuum	Rotary pump	0.01 Torr
	Heat	Source	Halogen lamp
		Range	0–650 °C
	Thermal couple	K-type	Indenter; Specimen; Stage

draft, reported in previous research, were prevented by vacuum conditions [17–19]. A radiation shield and cool water circulation were set up around the stage and around the connecting shaft of IIT. All specimen faces were heated equally by the halogen lamp. Thermocouples enabled real-time temperature detection in the indenter, specimen surface, and stage, and the movement of the stage was controlled externally. Fig. 1 and Table 1 show the features of the HTIIS and its specifications.

One experiment was performed to calibrate the frame compliance, as caused by elastic deformation of HTIIS during indentation [1,2]. A standard hardness specimen (HV300) was used, and the Vickers indenter had face-to-face angle 136°. The indentation rate was constant at 0.3 mm/min [8,15,16] and the indentation depth was 80 μm. The temperature was varied at 100 °C intervals from room temperature to 600 °C in vacuum condition, and the indentation load–depth curve was measured five times at each temperature. Stiffness was determined from the data at the start of the unloading curve.Table 2.

Another experiment was performed under the same conditions to evaluate the contact area using HTIIS for nine kinds of carbon steels: SKS3, S45C, SKH51, SUJ2, SKD61, SK3, SKD11, SCM4 and SCM21 at 25 °C, 200 °C, 400 °C and 600 °C. The specimen surface was polished to 1 μm.

Lastly conventional high-temperature Vickers hardness testing was performed to verify HTIIS experimental results for the same nine carbon steels. AVK-HF (Akashi, Japan) was used for conventional Vickers hardness testing at 25 °C, 200 °C, 400 °C and 600 °C at the Technology Innovation Center for Fine Ceramics (FCTIC, Korea).

Table 2
Mechanical properties of specimens.

	E (GPa)	YS (MPa)	UTS (MPa)	n	HV
SKS3	210	435	756	0.22	195
S45C	212	363	774	0.26	171
SKH51	223	295	784	0.26	222
SUJ2	217	404	822	0.24	199
SKD61	214	371	781	0.24	201
SK3	207	315	707	0.26	165
SKD11	217	343	808	0.26	230
SCM4	235	723	994	0.13	229
SCM21	194	271	653	0.22	137

3. Results and discussion

The measured indentation depth when the load is applied is affected by forces acting normal to the specimen and by forces of the same size acting in the opposite direction to the equipment. Hence errors can arise in the measured indentation depth. Determining the deformation from the forces acting normal to specimen is called calibration of frame compliance.

Fig. 2 shows the total frame compliance (C_{total}) of the HTIIS from room temperature to 600 °C. Following in Oliver and Pharr's footsteps [1,2], C_{total} can be determined from the stiffness by analyzing data from the unloading curve. The value of C_{total} increases with increasing temperature because the shaft of HTIIS and the specimen are heated at the same time by the halogen lamp, so the elastic modulus of shaft and specimen are reduced to facilitate

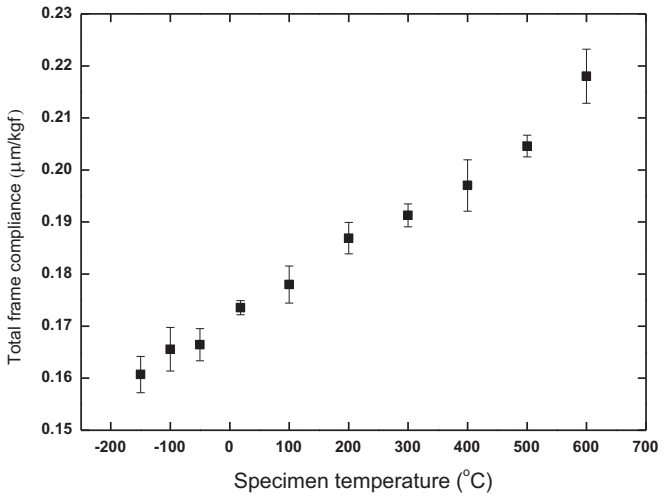

Fig. 2. Total frame compliance C_{total} (μm/kgf) at 25–600 °C.

the deformation. In other words, the elastic modulus of both shaft and specimen decreases with increasing temperature: C_{total} has an inverse relationship with elastic modulus and thus tends to increase linearly. (Oliver and Pharr could consider C_{total} as constant because their work was performed only at room temperature.) Thus, through the relationship between the calculated C_{total} and the observed contact area, the indentation depth can be calibrated by calculating the frame compliance (C_{frame}) as in Eq. (1) [1,2]:

$$C_{total} = C_{frame} + \frac{\sqrt{\pi}}{2E_r}\cdot\frac{1}{\sqrt{A_c}} \quad (1)$$

where C_{total} is the total frame compliance of the equipment, E_r is the reduced elastic modulus and A_c is the contact area. Extension of this method in this study confirms that the value of C_{total} is linear with temperature, so the indentation depth at high-temperatures can be corrected using Eq. (2) derived from the data fitting in Fig. 2:

$$C_{total} = 6.763 \times 10^{-5}\cdot T(^{\circ}C) + 0.172 \quad (2)$$

Eq. (2), proposed in this study, gives the compliance change of all modules of HTIIS as a function of temperature. In addition, it was difficult to observe the contact area directly in the chamber during the high-temperature experiments. Therefore, assuming that the hardness value that normalizes the load to the contact area is always constant, it is applied to the equation as in Eq. (3), by replacing A_c with the ratio of the hardness (H) and maximum load (L_{max}):

$$C_{total} = C_{frame} + \frac{\sqrt{\pi}}{2E_r}\cdot\frac{\sqrt{H}}{\sqrt{L_{max}}} \quad (3)$$

Another issue in studying HTIIS is precise determination of the contact area, since this is used as a basic parameter in evaluating mechanical properties.

Fig. 3 shows that h_c is the vertical depth along which contact is made, and h_m is the depth at maximum load. h_f is the final depth which occurs after unloading; elastic recovery of material. Contact area is derived from indentation depth. Thus, to determine an accurate indentation depth, it is important not only to calibrate the frame compliance but also to quantify the effect of pileup, i.e. atoms accumulating on the periphery of the indenter during plastic deformation. According to previous studies, ignoring the pileup effect can lead to differences in contact area of up to fifty percents [22,23]. Various studies have been conducted to quantify the pileup effect. Among these are studies using f as a pileup calibration factor, where f is defined in Eq. (4) and it is a dimensionless factor:

$$f = \frac{h_c}{h_m} \quad (4)$$

The factor f expresses the height of the pileup as the ratio of the

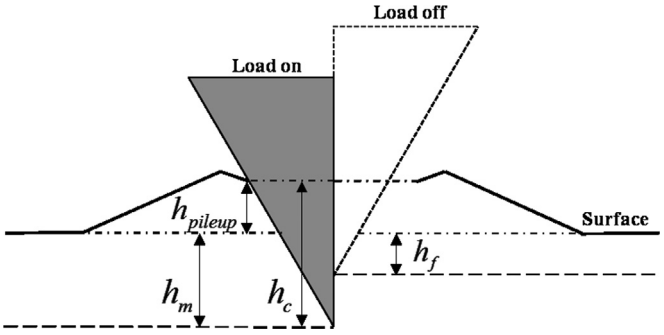

Fig. 3. Contact morphology with pile-up.

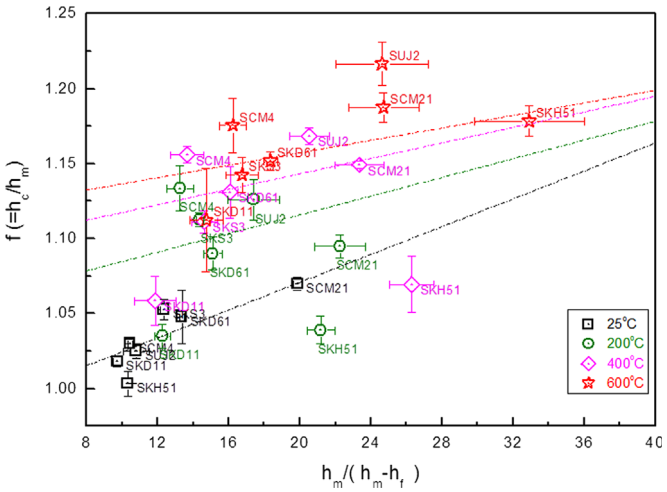

Fig. 4. Relationship of f and $h_m/(h_m - h_f)$ at 25 °C, 200 °C, 400 °C, 600 °C.

real indentation depth (h_c), which is considered to be from plastic accumulation, and the maximum indentation depth (h_m), which can be measured from the equipment. Previous studies have reported that f is associated with material properties and can be expressed using tensile parameters as well as indentation parameter as in Eq. (5) [3,12,14–16]:

$$f \approx \frac{\sigma_y}{E} \approx \frac{H}{E} \approx \frac{W_e}{W_{total}} \approx \frac{h_m}{h_m - h_f} \quad (5)$$

However, so far, only at room temperature have studies of pileup been performed for quantification. At high-temperatures, yield strength, elastic modulus, and work-hardening values are generally reduced, so it can be inferred that the effect of increasing temperature should be reflected.

Fig. 4 shows the increase in pileup with increasing temperature and the relation between pileup and the indentation parameter and demonstrates the linearity between pileup and indentation parameter, as found in previous room-temperature studies. However, what happens when temperature increases? As temperature increases, the slope of this linearity gradually decreases and the values of intercept increase dramatically:

$$f_{(T)} = A_{(T)}\cdot\left(\frac{h_m}{h_m - h_f}\right) + B_{(T)} \quad (6)$$

Here h_m is maximum indentation depth and h_f is final indentation depth. As shown in Eq. (6), the slope ($A_{(T)}$) is the ratio of the variation of indentation parameter against the variation of increasing pileup with increasing temperature. In this study, h_m is constant at 80 μm. Thus, the $A_{(T)}$ is related to the indentation variable ($h_m - h_f$), which represents the amount of elastic recovery after unloading. Fig. 5 shows that the change of slope at each temperature in Fig. 4 relates to the amount of elastic recovery in the specimen; in other words, at each temperature the slope could change depending on whether or not the specimens show large elastic recovery. For instance, comparing the slope and elastic recovery at each temperature in SCM21 and SKD61 in Figs. 4 and 5 show that the amount of elastic recovery decreases with increasing temperature. The decrease in elastic recovery is related to pileup, so this confirms that the slope is gradually decreased.

Note that in the case of S45C and SK3 in Fig. 6, the relation of pileup and indentation parameter does not seem to be linear, unlike in Fig. 4. The S45C and SK3 specimens undergo a phenomenon called blue shortness or blue brittleness, which usually occurs from 200 °C to 400 °C: the surface color becomes blue and

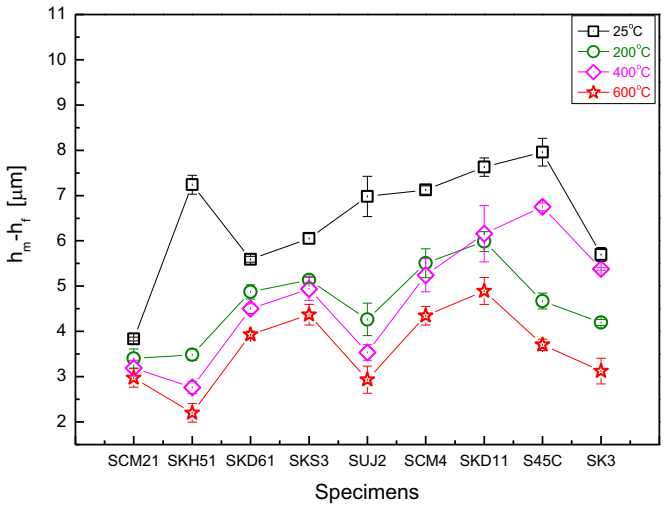

Fig. 5. Elastic recovery $h_m - h_f$ (μm) for specimens at 25 °C, 200 °C, 400 °C, 600 °C.

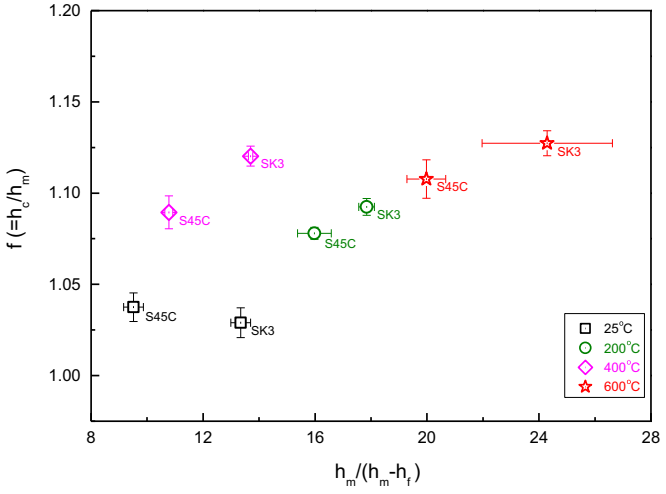

Fig. 6. S45C and SK3: relationship of f and $h_m/(h_m - hf)$ at 25 °C, 200 °C, 400 °C, 600 °C.

hardness or strength temporarily increases. The results in Fig. 6 may confirm the experimental results of Riaz and Atiqah [24]. This phenomenon is relevant to deformation behavior of metal at high-temperatures. Metals under short-term deformation at high-temperatures can be hardened due to easy dislocation proliferation and cross-slip, and can at the same time recover due to re-crystallization or dislocation extinction or rearrangement. Hardening and recovery offset each other at once during high-temperature deformation, so that elastic–plastic deformation proceeds in balance. However, in this specific temperature range, the offset and the balance no longer occur, hardening dominates recovery, and consequently the metal is strengthened [25]. Therefore, the hardness value of S45C and SK3 at 400 °C becomes higher than the value at 200 °C.

Fig. 4 shows that the value of the intercept ($B_{(T)}$) increases with increasing temperature. This is because fitting is carried out in one dimension, as in Eq. (6). The increase in pileup with increasing temperature could be also represented as an increase of $B_{(T)}$. Thus, this study proposes a new equation calibrating pileup effect by taking temperature into account:

$$f_{(T)} = [\alpha\cdot(^{\circ}C) + \beta]\cdot\left(\frac{h_m}{h_m - h_f}\right) + [\gamma\cdot(^{\circ}C) + \delta] \quad (7)$$

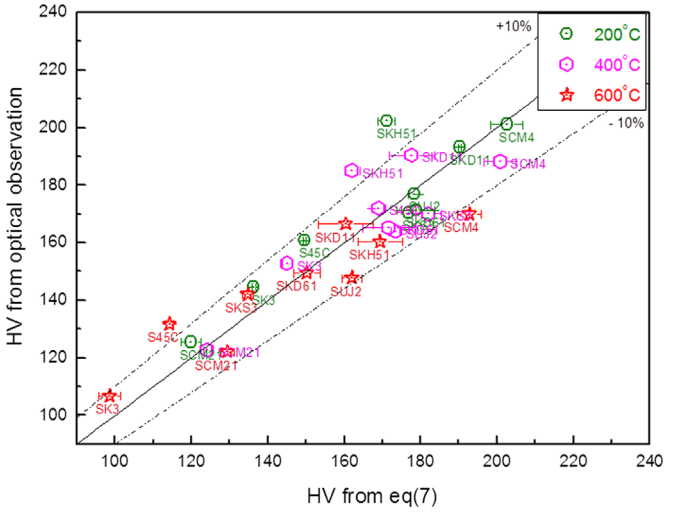

Fig. 7. Comparison of hardness results by conventional method and by HTIIS using Eq. 7.

Where, $[\alpha\cdot(^{\circ}C)+\beta]$ is $[-4.225\cdot10^{-6}\cdot(^{\circ}C)+0.004]$ and, $[\gamma\cdot(^{\circ}C)+\delta]$ is $[2.322\cdot10^{-4}\cdot(^{\circ}C)+0.989]$. Eq. (7) is derived by fitting from the data in Fig. 4 about a decreased slope and an increased intercept aspect with increasing temperature. Using Eq. (7) yields the real indentation depth (h_c), and thus makes it possible to determine the real contact area at high-temperature.

Fig. 7 shows hardness results as evaluated by HTIIS using Eq. (7) and by conventional methods (optical observation). Conventional Vickers hardness is defined in Eqs. (8) and (9) by considering the geometrical shape of indenter [16,26]:

$$HV(^{\circ}C) = \frac{L_{max}}{26.43\cdot(h_c^2)} \quad (8)$$

$$h_c = \frac{d}{2\sqrt{2}\,\tan\theta^{\circ}} \quad (9)$$

where L_{max} is the maximum load, and θ is the half angle of the Vickers indenter here 68 ° and d is the diagonal length of the indentation mark. The relationship between the diagonal and contact depth at high-temperature is defined here by using Eq. (7) and $f_{(T)}$; where $(h_c = f_{(T)}\cdot h_{max})$. Generally HV can be evaluated by measuring diagonal length of indentation mark directly even high-temperature.

However, HV can also be evaluated by measuring indentation depth and considering geometrical shape of indenter. Because contact area is a function of indentation depth and HV is a function of the maximum load and contact area. It can be seen that the Fig. 7 compares HV resulting from calibrated and un-calibrated indentation depth (h_c). In other words, if $h_c = h_{max}$ is derived from d by optical observation at high-temperature, the conventional method is indicated. But, if $h_c = f_{(T)}\cdot h_{max}$ is derived from Eq. (7), the pileup calibration method at high-temperature studied here is meant.

The results match within 10% error. It is difficult, however, to agree that Eq. (7) describes the pileup behavior completely at high-temperature, even though the hardness results agree well. Because a peculiar hardening behavior occurs at high-temperature (blue brittleness in Fig. 6), in order to solve this problem, the effect of temperature on the hardening behavior, which has been ignored in some in previous studies, must be studied in more detail.

4. Conclusions

This study investigates the real contact area, which is a basic indentation parameter in evaluating various mechanical properties at high-temperatures, using a newly constructed high-temperature instrumented indentation system (HTIIS). The elastic deformation of the HTIIS was calibrated according to increasing temperature. Pileup behavior was measured with changing temperature and was quantified using an indentation parameter. The hardness value yielded by the proposed pileup calibration factor $f_{(T)}$ for high-temperatures is in agreement within 10% error with conventional high-temperature hardness testing.

Acknowledgment

This work was supported by the Engineering Research Center of Excellence Program of Korea Ministry of Science, ICT & Future Planning (MSIP)/National Research Foundation of Korea (NRF) (Grant NRF-2015R1A5A1037627).

References

[1] W.C. Oliver, G.M. Pharr, An improved technique for determining hardness and elastic-modulus using load and displacement sensing indentation experiments, J. Mater. Res. 7 (1992) 1564.
[2] W.C. Oliver, G.M. Pharr, Measurement of hardness and elastic modulus by instrumented indentation: Advances in understanding and refinements to methodology, J. Mater. Res. 19 (2004) 3.
[3] A. Bolshakov, G.M. Pharr, Influences of pileup on the measurement of mechanical properties by load and depth-sensing indentation techniques, J. Mater. Res. 13 (1998) 1049.
[4] Y.-H. Lee, D. Kwon, Estimation of biaxial surface stress by instrumented indentation with sharp indenters, Acta Mater. 52 (2004) 1555.
[5] S.I. Bulychev, V.P. Alekhin, M.Kh Shorshorov, A.P. Ternovskii, Mechanical properties of materials studied from kinetic diagrams of load versus depth of impression during microimpression, Prob. Prochn. 9 (1976) 79.
[6] J.C. Hay, A. Bolshakov, G.M. Pharr, A critical examination of the fundamental relations used in the analysis of nanoindentation data, J. Mater. Res. 14 (1999) 2296.
[7] E.G. Herbert, G.M. Pharr, W.C. Oliver, B.N. Lucas, J.L. Hay, On the measurement of stress-strain curves by spherical indentation, Thin Solid Films 398–399 (2001) 331.
[8] J.S. Lee, J.I. Jang, B.W. Lee, Y. Choi, S.G. Lee, D. Kwon, An instrumented indentation technique for estimating fracture toughness of ductile materials: A critical indentation energy model based on continuum damage mechanics, Acta Mater. 54 (2006) 1101.
[9] S. Suresh, A.E. Giannakopoulos, A new method for estimating residual stresses by instrumented sharp indentation, Acta Mater. 465 (1998) 755.
[10] K.L. Johnson, Contact Mechanics, Cambridge University Press, Cambridge, UK, 1985.
[11] J.-H. Ahn, Y. Choi, D. Kwon, Evaluation of plastic flow properties of materials through the analysis of indentation load–depth curve, Korean Inst. Met. Mater. 38 (2000) 16067.
[12] Y.T. Cheng, C.M. Cheng, Relationships between hardness, elastic modulus, and the work of indentation, Appl. Phys. Lett. 73 (1998) 614.
[13] Y.T. Cheng, C.M. Cheng, What is indentation hardness, Surf. Coat. Technol. 133–134 (2000) 417.
[14] J. Alcala, A.C. Barone, M. Anglada, The influence of plastic hardening on surface deformation modes around Vickers and spherical indents, Acta Mater. 48 (2000) 3451.
[15] Y. Choi, H.S. Lee, D. Kwon, Analysis of sharp-tip-indentation load-depth curve for contact area determination taking into account pile-up and sink-in effects, J. Mater. Res. 19 (2004) 3307.
[16] S.K. Kang, J.Y. Kim, C.P. Park, H.U. Kim, D. Kwon, Conventional Vickers and true instrumented indentation hardness determined by instrumented indentation test, J. Mater. Res. 25 (2010) 2.
[17] C.A. Schuh, C.E. Packard, A.C. Lund, Nanoindentation and contact mode imaging at high-temperatures, J. Mater. Res. 21 (3) (2006) 725.
[18] B.D. Beake, J.F. Smith, High-temperature nanoindentation testing of fused silica and other materials, Philos. Mag. A82 (2002) 2179.
[19] J.F. Smith, S. Zheng, High-temperature nanoscale mechanical property measurement, Surf. Eng. 16 (2000) 143.
[20] B.N. Lucas, W.C. Oliver, Indentation power-law creep of high purity indium, Metall. Mater. Trans. 30A (1999) 601.
[21] C.A. Schuh, J.K. Mason, A.C. Lund, Quantitative insight into dislocation nucleation from high-temperature nanoindentation experiments, Nat. Mater. 4 (2005) 617.
[22] Y.Y. Lim, A.J. Bushby, M.M. Chaudhri, Nano and macro indentation studies of polycrystalline copper using spherical indenters, Mater. Res. Soc. Symp. Proc. 522 (1998) 145.
[23] Y.Y. Lim, M.M. Chaudhri, Y. Enomoto, Accurate determination of the mechanical properties of thin aluminium films deposited on sapphire flats using nanoindentation, J. Mater. Res. 14 (1999) 2314.
[24] M. Riaz, N. Atiqah, A study on the mechanical properties of S45C medium type carbon steel specimens under lathe machining and quenching condition, IJRET 3 (2014) 12.
[25] E. George, Dieter: Mechanical Metallurgy University of Maryland, third edition, McGraw-Hill Inc, USA, 1986.
[26] ISO/FDIS 14577-1, Metallic Materials-Instrumented Indentation Test for Hardness and Materials Parameters; Part 1, Test Method, International Organization for Standardization, Geneva, Switzerland, 2002.